Rho-dependent formation of epithelial "leader" cells during wound healing

T. Omelchenko*†, J. M. Vasiliev‡§, I. M. Gelfand¶, H. H. Feder†, and E. M. Bonder*†‖

*Program in Cellular and Molecular Biodynamics and †Department of Biological Sciences, Rutgers University, Newark, NJ 07102; ‡Belozersky Institute of Physico-Chemical Biology, Moscow State University, Moscow 119899, Russia; §Oncological Scientific Center of Russia, Moscow 115478, Russia; and ¶Department of Mathematics, Rutgers University, Piscataway, NJ 08854

Contributed by I. M. Gelfand, July 14, 2003

The motile behavior of epithelial cells located at the edge of a large wound in a monolayer of cultured cells was analyzed. The initial cellular response is alignment of the edge with an accompanying formation of tangential marginal actin bundles within individual cells positioned along the wound edge. Later, coherent outgrowths of cell masses occur by the formation of special "leader" cells at the tops of outgrowths and "follower" cells along the sides. Leader cells exhibit profound cytoskeletal reorganization, including disassembly of marginal bundles, the realignment of actin filament bundles, and penetration of microtubules into highly active lamellae. Additionally, cell–cell contacts acquire radial geometry indicative of increased contractile tension. Interestingly, leader cells acquire a cytoskeletal organization and motility typical of fibroblasts. IAR-2 cultures stably transfected with a dominant-negative mutant of RhoA or treated with Rho-kinase inhibitor Y-27632 transformed most edge cells into leader-like cells. Alternatively, transfection of cells with constitutively active RhoA suppressed formation of leaders. Thus, expansion of the epithelial sheet involves functional differentiation into two distinct types of edge cells. The transition between these two patterns is controlled by Rho activity, which in turn controls the dynamic distribution and activity of actin filament bundles, myosin II, and microtubules.

Trinkaus (1) wrote that "spreading of adhesive sheets, often covering a considerable expanse, is a commonplace morphogenetic movement in both embryos and adults." Our understanding of the cellular and molecular mechanisms of epithelial wound healing and related morphogenetic processes, such as dorsal closure of the epidermis in *Drosophila*, has recently made significant progress (2–4). An important stage in the movement of epithelial sheets is alignment of edge cells along the wound/opening boundary and formation of tangential marginal bundles of actin filaments. The ends of marginal bundles are associated with the E-cadherin/β-catenin adhesion complex that forms cell–cell adherens junction (3, 4). This structural organization essentially forms a ring around the wound circumference and functions as a "purse string" facilitating wound closure. In such experiments, migration of epithelia occurs into relatively small, circular holes or wounds.

The importance of the Rho family of small GTP-ases controlling cytoskeletal organization is well established (reviewed in refs. 5 and 6). Briefly, Rho family members have been shown to regulate contractile activity, stress fiber formation, filopodial extension, and lamellipodial activity. For example, dorsal closure during *Drosophila* development requires formation of the actin cable in edge cells and closure is abnormal in embryos expressing mutations affecting Rho1 and myosin II (7–9).

In the present report, we examined the coordinated migration of epithelial cells along the edge of wounds that were in effect infinitely large and thus precluded the formation of a circumferential purse string. Under these conditions, it was found that after alignment of edge cells the border of the monolayer formed large multicellular outgrowths with specialized leader cells at the top and follower cells at the sides. Formation of leader cells involved loss of marginal actin bundle and development of a large leading lamella with microtubules extending out to the active edge. The overall organization of the cytoskeleton and cell–cell contacts in leader cells is similar to those exhibited by fibroblast-like cells. We also examined the role of RhoA protein in formation of leader and follower cells. Transfection of constitutively active RhoA suppressed formation of leaders, whereas suppression of RhoA led to transformation of almost all edge cells into leaders. Lastly, the possible mechanisms by which Rho may control these transformations and the relevance of these phenomena to *in vivo* physiological and pathological morphogenetic processes are discussed.

Materials and Methods

Cell Culture and Generation of Stable Cell Lines. IAR-2 rat liver epithelial cells (10) were maintained at 37°C in 5% CO_2 incubator in DMEM supplemented with 10% FCS (Atlanta Biologicals, Norcross, GA) with or without antibiotics. Plasmids encoding constitutively active [enhanced GFP (EGFP)-RhoA Q63L] or dominant-negative (EGFP-RhoA T19N) recombinant RhoA have been described (11) and were kindly provided by G. Bokoch (The Scripps Research Institute, La Jolla, CA). The plasmid pEGFP-Tub was obtained from CLONTECH. Cells were transfected by using Lipofectamine reagent (Invitrogen Life Technologies) according to the manufacturer's specifications. Cells were isolated by selection for resistance to G418, and individual fluorescent colonies were picked after direct, microscopy-based screening (12).

Time-Lapse Video Observations. Confluent cultures of cells were grown in CO_2-independent medium (Invitrogen Life Technologies) on etched glass coverslips (Bellco Glass, Vineland, NJ) for 48 h. Wounds were made by removing half of the monolayer with a sterile razor blade. Time-lapse video observations of live cells were started between 0 and 72 h after wounding. For some experiments, wounded cells were incubated with either 1 or 10 μM Y-27632 (Calbiochem), added immediately after wounding. Y-27632 is a highly selective inhibitor of Rho kinase (13). Observations were made by using a Nikon Diaphot 300 microscope equipped with a Plan $\times$10 (numerical aperture 0.3), Plan $\times$20 (numerical aperture 0.4), phase-contrast optics, and a temperature-controlled stage. Image acquisition was controlled by METAMORPH software (Universal Imaging, West Chester, PA). Time-lapse video differential interference contrast microscopy was performed on a Zeiss Axiophot (14).

For imaging of EGFP-fluorescence, cells were maintained in CO_2-independent medium containing 0.3 units/ml Oxyrase oxygen scavenging system (EC Oxyrase; Oxyrase, Mansfield, OH), and images were collected by using a Bio-Rad MRC 1024 laser scanning confocal microscope.

Abbreviation: EGFP, enhanced GFP.

‖To whom correspondence should be addressed. E-mail: ebonder@andromeda.rutgers.edu.

www.pnas.org/cgi/doi/10.1073/pnas.1834401100

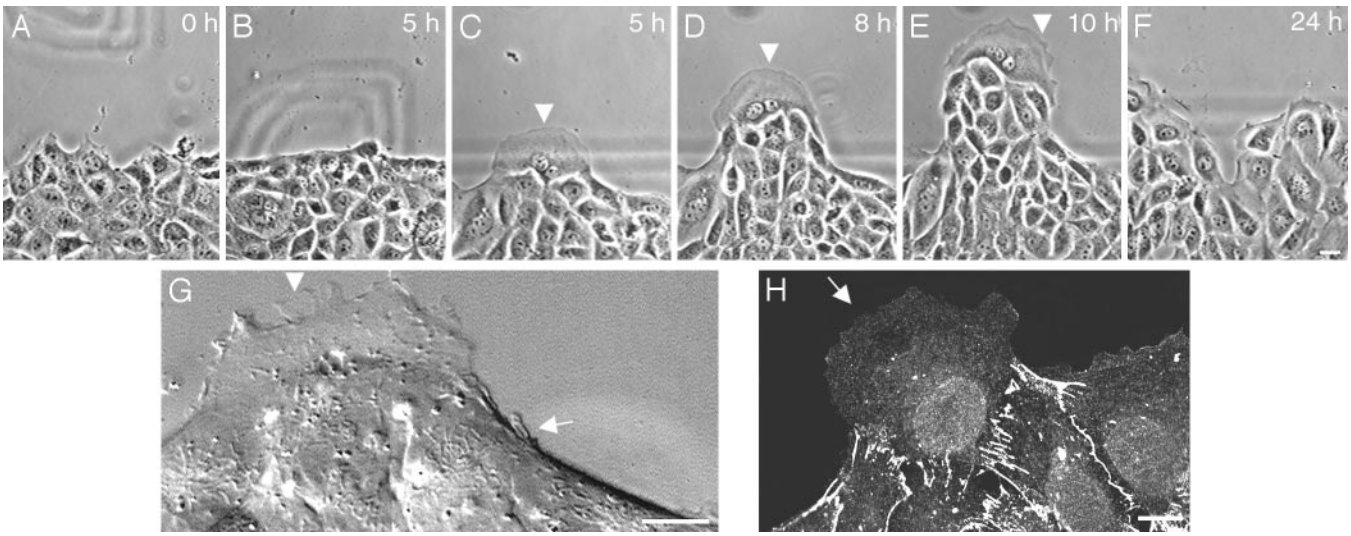

Fig. 1. Movement of the epithelial sheet of IAR-2 culture into the wound. Phase contrast micrographs demonstrate nonaligned sheet (*A*), aligned cells at the edge (*B*), and a ''leader'' (arrowheads in *C–E*) initiated progressively growing protrusion. (*F*) Leaders forming along the lateral edge of outgrowths. (*G*) Wide lamellipodium formed by leader (arrowhead) and small lamelipodia (arrow) formed by its ''follower'' documented by differential interference contrast microscopy. (*H*) E-cadherin staining showing altered radial cell–cell contacts at the sides of leader. Arrow indicates the active edge of the leader. (Bars = 20 μm in *A–F* and 10 μm in *G* and *H*.)

Immunofluorescence Microscopy. For simultaneous localization of actin and microtubules, cells were fixed as described (15) and stained with mouse anti-tubulin antibody IgG1 clone DM1α (Sigma; 1:50 dilution) and rhodamine-phalloidin (Molecular Probes; 1:50 dilution). E-cadherin staining was carried out as described (16). For other staining, cells were rinsed in PBS and fixed in PBS containing 3.7% formaldehyde, permeabilized for 1 min with 0.5% Triton X-100 in PBS, and stained with mAbs raised against β-catenin, paxillin (BD Transduction Laboratories, Lexington, KY; 1:50 dilution), or polyclonal antibodies raised against fibronectin and laminin (kindly provided by A. Ljubimov, Cedars-Sinai Medical Center, Los Angeles; 1:25 dilution) and/or rhodamine-phalloidin to label actin. All primary antibodies were detected by using anti-mouse Alexa Fluor 488- or anti-mouse or anti-rabbit Alexa Fluor 568-conjugated secondary IgG antibodies (Molecular Probes; 1:200 dilution). Fluorescence images were collected by using the Bio-Rad MRC 1024 laser scanning confocal microscope system.

Pseudopodial Activity. Mean rates of protrusions and retractions of pseudopodia were quantitated as described (17).

Results

Dynamics of Cell Migration at the Edge of a Large Wound. Immediately after wounding, the edges of wounds had rugged contours, with edge cells having different shapes and orientation (Fig. 1*A*). Over the first 1–2 h, edge cells extended lamellas toward the wound, and eventually their contours became smooth, the cells acquired triangular or fusiform shape oriented toward the edge and the cells exhibited decreased lamellar activity (Fig. 1*B*). Interestingly, multicellular outgrowths 4–6 cells in width and up to 6–10 cells in length started to form 4–6 h after wounding (Fig. 1 *D* and *E*). The first stage of formation involved development of small ''mounds'' that included one or rarely two ''leader'' cells with large lamellas positioned at the top of the mound (Fig. 1 *C* and *D*). Leader cells retained contact along their basolateral surfaces with ''follower'' cells that were oriented toward the leaders. At 6 h, the mean rates of pseudopodial protrusion for leaders were three times higher than those of their immediate neighbor followers (see Table 1 and Fig. 1*G*). Lamellar activity of leaders appeared to advance the mounds forward, thereby creating longer outgrowths that extended into the wound space (Fig. 1*E*). After 24 h, the contour of the edge became very irregular as some cells at the bottoms and the sides of outgrowths were transformed into leader cells (Fig. 1*F*).

Cytoskeletal Reorganizations in Edge Cells. Immediately after wounding, nonaligned edge cells had no marginal bundles, straight actin bundles in the cytoplasm were oriented in multiple directions, and microtubules filled the entire cytoplasm (Fig. 2). Starting 2–3 h after wounding, marginal bundles started to assemble at approximately the same time as edge cells began to align (Fig. 2*B*). Microtubules in these cells were spread through-

Table 1. Mean rates of protrusion and retraction of pseudopodia of the edge cells

	Rate, μm/min ± SEM	
Cells (*n*)	Protrusions	Retractions
Aligned untreated cells (10)*	0.9 ± 0.1	0.8 ± 0.1
Pairs of untreated cells†		
Cell I, leader (10)	1.4 ± 0.2	0.4 ± 0.05
Cell II, follower (10)	0.4 ± 0.05	0.3 ± 0.07
Pairs of dominant-negative RhoA cells†		
Cell I (5)	1.3 ± 0.3	0.44 ± 0.06
Cell II (5)	1.2 ± 0.13	0.47 ± 0.09
Pairs of constitutively active RhoA cells†		
Cell I (5)	0.3 ± 0.03	0.2 ± 0.01
Cell II (5)	0.3 ± 0.02	0.2 ± 0.02
Cells incubated with Rho-kinase inhibitor (7)*	1.4 ± 0.05	0.7 ± 0.1

The rates were expressed as μm/min ± SEM. In cultures with outgrowths, we measured pairs of edge cells: leaders at the top of protrusion and the nearest lateral follower. In dominant-negative and constitutively active RhoA cultures, differentiation of two cell types was not observed, and pairs of neighbor edge cells were picked at random for measurements.
*Two-hour wound.
†Six-hour wound.

CELL BIOLOGY

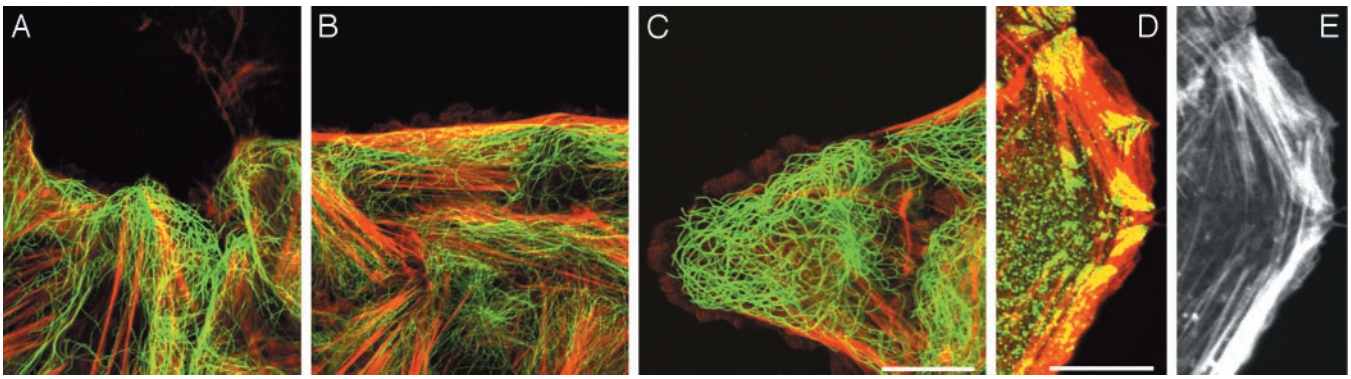

Fig. 2. Localization of actin, microtubules and paxillin in edge cells. Cells were double-stained for actin (red) and microtubules (green in *A–C*) or paxillin (green in *D*). (*A* and *B*) Irregular distribution of actin bundles and microtubules at the edge immediately after wounding (*A*); in aligned cells (*B*), marginal bundle formed and microtubules did not cross this bundle. (*C*) Marginal bundles were present in the followers but absent in the leader. (*D*) In leader cells the marginal bundles became decomposed and triangular focal contacts were seen at the ends of fragments of the bundle. (*E*) Actin fluorescence of the same field as in *D*. (Bars = 10 μm.)

out the cytoplasm except in the anterior portion of the cell, where the tangential marginal bundle and active lamellipodia were located (Fig. 3*A*).

During transformation of edge into leader cells, the marginal bundles started to fragment and their remnants formed straight bundles located along the sides of the cell (Fig. 2 *C* and *D*). During this time period, other bundles of actin filaments became oriented perpendicular to the free edge of the cell. Follower cells in cell–cell contact with leaders usually retained their normal overall cytoskeletal organization.

Upon disassembly of marginal bundles, peripheral microtubules now penetrated out into the actively growing and retracting lamellipodia (Figs. 2*C* and 3 *A* and *B*). Real-time observations of cellular microtubules labeled with EGFP-Tub (Fig. 3 *A* and *B*) established that individual microtubules grew repeatedly and often into the peripheral part of the cytoplasm and penetrated into ruffling lamellipodia of leader cells. This was in contrast to follower cells, with intact marginal bundles, where growth of microtubules into the active lamellipodial edge was a very rare occurrence (Fig. 3*A*). In cells with marginal bundles, microtubules that grew beyond the marginal bundle soon stopped and retracted away from the edge.

Staining for β-catenin identified the presence of tangential junctional assemblies in all interior parts of the monolayer (Fig. 1*H*; also see refs. 14 and 16). Contacts between leader cells and their follower neighbors became discontinuous and acquired radial orientation perpendicular to the edges (Fig. 1*H*). Previously, it was shown that perpendicular orientation of cell–cell contacts stems from increased contractile activity of the actin cytoskeleton (14, 16). Focal contacts were localized to the ends of actin filament bundles in both leader and follower cells. Leader cells often formed peculiar large triangular focal contacts at their free edge and the contacts appeared to be associated with the ends of fragmented marginal bundles of actin filaments (Fig. 2 *D* and *E*). There was no detectable correlation between the presence of matrix proteins and the location of a cellular outgrowth along the wound edge (not shown).

Dynamics of Epithelium Expressing Dominant-Negative RhoA. Edge cells expressing the dominant-negative construct RhoA T19N failed to align after wounding and most developed large anterior lamellas (Fig. 4 *A* and *B*). Even after 6–12 h, most cells at an edge had large lamellas (≈80–85% of all edge cells as compared with ≈18–20% in control at 10 h). All of the edge cells possessed leader-type morphology, and there was no detectable formation of follower cells (Fig. 4 *A* and *B*). Cells behind the edge appeared randomly oriented and often detached from one another, creating gaps connected by narrow fibrils. Cells with very long tails were not observed, as has been reported for monocytes with inhibited Rho (18). The mean rates of lamellipodial protrusions in RhoA T19N cells at 6 h were similar to those measured for leader cells of control cultures (Table 1). After 48 h, organized outgrowths were not observed.

Edge cells expressing RhoA T19N did not possess marginal

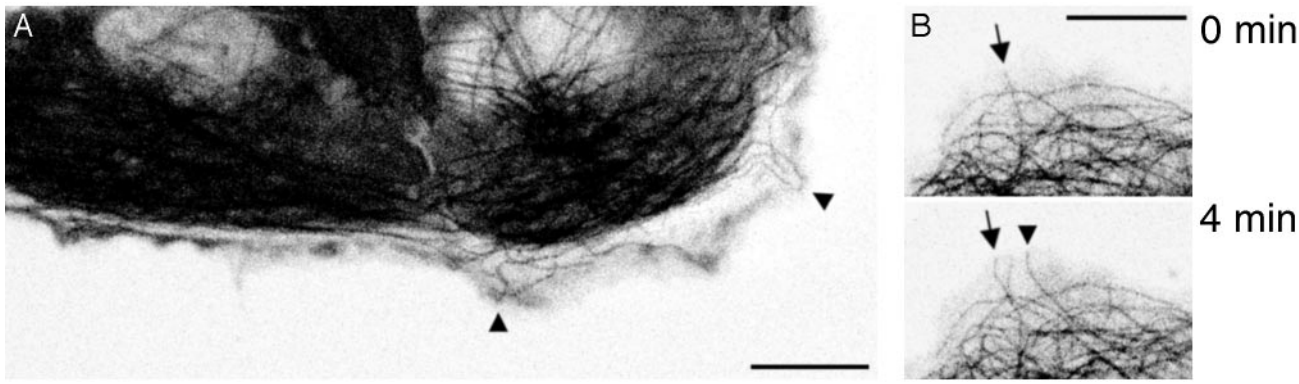

Fig. 3. Movement of microtubules in live edge cells expressing EGFP-tubulin. (*A*) Microtubules grew into lamella (arrowheads) of leader cells (right) but not into that of follower (left). (*B*) Individual microtubule of a leader cell penetrated to the active edge (arrow) and a newly formed microtubule (arrowhead) grew into the lamelipodium. (Bars = 10 μm.)

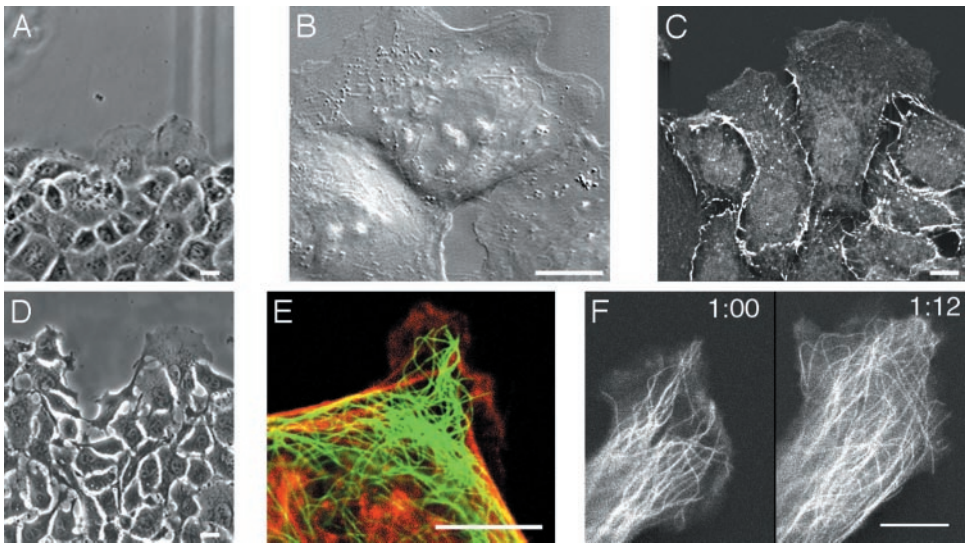

Fig. 4. Effect of transfection of IAR-2 cells with dominant-negative RhoA (*A–C*) or incubation with Y-27632 inhibitor of Rho kinase (*D–F*). (*A*) Phase contrast micrograph of epithelial sheet expressing dominant-negative RhoA demonstrates several leader-type cells with large lamellas at the edge. (*B*) Several wide lamellipodia formed by central cell and by its neighbor; note the hole between the cells. (*C*) E-cadherin staining revealed fragmented contacts. (*D*) Many cells with lamellas and processes were seen at the edge of 10 μM Y-27632-treated cells imaged by phase contrast microscopy. (*E*) The inhibitor caused disruption of the center of marginal bundle (red) and microtubules (green) penetrated through the opening in the bundle to ruffling edge. (*F*) Movements of microtubules near the edge of the extended lamellar process observed in live cell expressing EGFP-labeled tubulin and treated with 10 μM Y-27632 for 1 h. (Bars = 20 μm in *A* and *D* and 10 μm in *B*, *C*, *E*, and *F*.)

bundles of actin filaments; however, other actin bundles continued to form, but they were less numerous than in controls. Microtubules were present in all regions of the cytoplasm and often reached out into active lamellipodia. In those areas where cells were in physical contact with an adjacent cell, the tangential cell–cell contacts continued to persist but sometimes were fragmented (Fig. 4*C*).

Dynamics of Epithelium Treated with Rho-Kinase Inhibitor Y-27632. Rho kinase is one of the main downstream targets of RhoA signaling and it is known to participate in Rho signaling involved in actin–myosin II contractile activity. Within 10–60 min of exposure to 10 μM Y-27632, edge cells formed large lamellas and elongated narrow processes (Fig. 4*D*). Marginal bundles in most edge cells started to disassemble and fragment enabling microtubules to extend, between fragments of dispersed bundles, into the peripheral lamellipodia. Observation of fluorescently labeled tubulin in live cells demonstrated that microtubules grew into lamellipodia and into the expanding processes, usually within 1–2 min after formation of the lamellipodia (Fig. 4 *E* and *F*). Other characteristics were also similar to those observed in cells expressing the dominant negative RhoA T19N construct. Thus, diminished activity of RhoA or Rho kinase caused the induction of many edge cells to take on a leader-like morphology with similar changes to cytoskeletal organization.

Dynamics of Epithelium with Constitutively Active RhoA Construct. IAR-2 cells stably transfected with RhoA Q63L, a constitutively active construct, were prepared and used in the wound-healing assay. Edge cells and cells within the interior of the monolayer were less spread and more rounded than nontransfected control IAR-2 cells (Fig. 5*A*). Alignment of the edge cells was significantly delayed, taking 12–24 h and even then alignment was only partially completed (Fig. 5*B*). Leader cells possessing wide lamellas and no marginal bundles rarely formed (3–4% of all edge cells at 10 h as compared with 18–20% in controls).

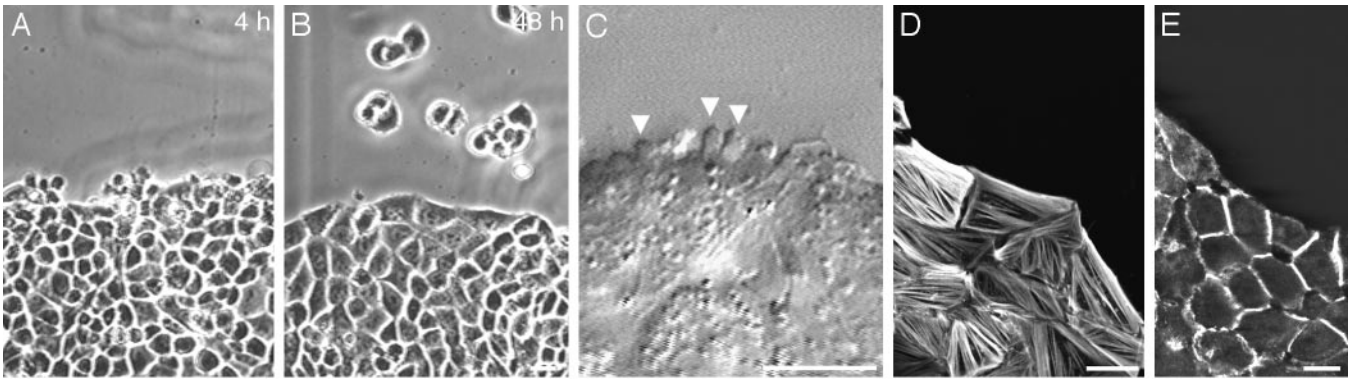

Fig. 5. Effect of transfection of IAR-2 cells with constitutively active RhoA. (*A*) Phase contrast micrograph shows that cells after 4 h of wounding had poorly aligned edge and no protrusions. (*B*) After 48 h, cell alignment was increased and numerous cell islands, at the free substrate, were formed. (*C*) Blebs (arrowheads) and small lamellipodia at the edge were observed by differential interference contrast microscopy. (*D*) Transfected cells stained for actin had marginal and central actin bundles. (*E*) Well developed tangential contacts revealed by β-catenin staining. (Bar = 20 μm in *B* and 10 μm in *C–E*.)

Typically, cells extended small lamellipodia and often formed and retracted small blebs (Fig. 5*C*) and the rate of protrusion/retraction was reduced relative to control, aligned cells (Table 1). Although cells near the wound remained in a monolayer, central parts of the epithelial sheet developed two to three layers of unspread nearly spherical cells. After 24 h, single cells and small islands of two to six cells were seen positioned on the substrate in the wound area at different distances from the edge of the wound (Fig. 5*B*). Occasionally, rounded cells were observed floating in the medium.

Constitutively active RhoA cells possessed numerous actin bundles including circumferential bundles at the cell periphery (Fig. 5*D*). Microtubules filled the central parts of the cytoplasm but did not penetrate to the periphery. Tangential E-cadherin and β-catenin staining contacts surrounded each cell in the monolayer (Fig. 5*E*).

Discussion

Formation and Function of Leader Cells During Migration of Epithelial Sheets. Wound healing along an epithelial sheet has typically been modeled as occurring by the progressive advancement of a uniform front of cells driven by "purse-string" contractile activity (1–9). This hypothesis has also been adopted to describe the mechanisms underlying migration of epithelial layers during embryonic morphogenesis (7, 9).

We examined wound healing of epithelial sheets in a culture system where the sheet moved not into a small wound, but into an infinitely long, vast substrate. As with purse string models, the initial response of the injured monolayer was to create a relatively uniform front of aligned edge cells. Shortly after alignment, the monolayer formed cellular outgrowths that advanced into the cell free wound. At the top of each outgrowth was a special leader cell possessing broad, highly active leading lamellas. The enhanced motile activity of leader cells appeared to pull their neighbor follower cells forward into the wound. With time, new leaders appeared along the sides of the outgrowth thereby leading to lateral expansion of the advancing outgrowth. The cycle of creating new outgrowths with new leaders and followers would eventually seal a large wound within a monolayer.

Cytoskeletal and Adhesion Junction Reorganizations Associated with Formation of Leader Cells. The most prominent features of transformation of an epithelial cell into a leader were the disassembly of the marginal bundle of actin filaments, formation of numerous, straight bundles of actin filaments oriented toward the free cell edge, and the expansion of a broad, active anterior lamella. The newly reorganized structure of the actin cytoskeleton was similar to what is routinely observed in fibroblasts. Transformation of epithelial cells into a more fibroblast-like phenotype is known to be induced by multiple soluble agents, e.g., by scatter factor protein (19–21) or by localized cell–cell contact with a fibroblast (22).

Leader epitheliocytes maintain numerous cell–cell adhesion contacts with follower cells; however, these contacts often acquire radial geometry, in contrast to typical tangential contacts observed in epithelial cultures. This transformation of contact geometry was observed (15) in epithelial IAR-2 cultures treated with nocodazole or phorbol ester to induce myosin driven contractile activity. Leader cells exhibit a similar local transformation suggesting the presence of enhanced tension along the advancing outgrowth. Most probably, extension and attachment of anterior lamella of leader cells produces a forward tension leading to reorientation of actin bundles (stress fibers) and cell–cell contacts. Consequently, the gradient of tension created by the leader cell pulls the followers into the outgrowth followed by subsequent active movement of neighbor cells.

As shown earlier (23), microtubules in single discoid epithelial cells radiate outward toward the circular marginal bundle where they can become aligned and run along the bundle rather than penetrate out into the lamella. In aligned edge cells, microtubules did not grow beyond the tangential bundles, whereas in an adjacent leader cell, with dispersed or fully disassembled marginal bundle, microtubules were observed throughout the anterior lamella. Treatment of cultures with the Rho-kinase inhibitor Y-27632 rapidly led to disorganization of marginal bundles followed by growth of microtubules through the gaps in the bundle with an accompanying expansion of lamellipodia. Thus, myosin-II-dependent contractile activity along the marginal bundles maintains bundle integrity, which in turn prevents access of microtubules to the edge of the cell where they might trigger localized polymerization of actin filaments (23).

The mechanism(s) enabling marginal bundles of actin filaments to function as a barrier preventing microtubule access to the cell edge is presently speculative. One possibility relies on the marginal bundle creating a simple physical barrier to the microtubules. Alternatively, because marginal bundles have been shown to undergo centripetal flow (24), this may provide a counter force that directs microtubule growth away from the cell edge (25). Consequently, marginal bundles appear to limit and guide microtubule growth, which indirectly functions to regulate lamellipodial activity (26–28).

Formation and Function of Leader Cells Are Rho-Dependent. To begin dissecting the molecular mechanisms regulating leader cell formation and function, we used IAR-2 cells transfected with the dominant-negative or constitutively active RhoA constructs, RhoA T19N and RhoA Q63L, respectively. Cultures of stably transfected cell lines expressing RhoA T19N never developed the characteristic of leader and follower outgrowths during wound healing. Most edge cells formed large lamellas, did not have numerous bundles of actin filaments, and started to lose lateral adherens contacts with neighboring cells. Furthermore, edge cells did not influence the shape or cytoskeleton organization of internal neighbor cells, presumably because of diminished ability to develop contractile tension, through a myosin II pathway. This conclusion was supported by treating IAR-2 cells with Y-27632, a selective inhibitor of Rho kinase.

In contrast to the well-spread RhoA T19N cells, edge cells and interior cells of cultures expressing constitutively active RhoA Q63L were rounded and appeared highly contracted with abundant actin bundles, including marginal bundles. After wounding, these cultures showed greatly delayed alignment and we did not observe formation of leaders and outgrowths. Although most cells within the culture exhibited normal-looking tangential cell–cell contacts, cells did detach from the monolayers and were released into the medium. Most probably, constitutively active RhoA activity leads to increased contractile tension, leading to inhibition of spreading, and subsequent detachment from the substrate.

The results of overexpression of dominant-negative and constitutively active variants of RhoA establish that successful formation of outgrowths requires spatial and temporal coordination of RhoA activity across the epithelial edge. Too many leaders result in a disorganized, nondirected epithelial sheet, whereas the absence of leaders in RhoA Q63L-expressing cells creates a stagnant sheet, both of which prevent efficient wound healing.

How is the formation of leaders triggered and regulated? Staining for fibronectin and laminin did not reveal any correlation between the presence of matrix structures on the substrate and the sites of leader cell and/or outgrowth formation. Therefore, it is unlikely that outgrowth of the leader lamella is associated with prior accumulation of extracellular matrix molecules that might have locally guided specific edge cells. In our experiments, leader cell formation may be a random process;

however, in general, transformation of epitheliocytes into fibroblast-like leaders is probably determined by external cues, such as soluble molecules or contact with other cells (19–22).

Conclusion

Contractile activity within the actin cytoskeleton in interaction with microtubules plays a central role in regulation of two major morphogenetic processes performed by edge cells of the epithelial sheet during the process of epithelial sheet expansion. The first of these processes, edge alignment, standardizes the relative position and organization of edge cells. The second process, formation of leaders and outgrowths, in contrast, creates a complex system of competing and interacting cells with different morphologies and different roles in coordinating movement of the sheet.

The mechanism of alignment involves a complex signaling network leading to appropriate organization of "purse string" actin bundles and E-cadherin contacts (7–9). Formation of leaders may involve signaling cascades similar to those acting during epithelio-mesenchymal transformation in embryonic development (19–21).

Formation of leaders observed in epithelial sheets *in vitro* may have its counterparts in physiological and pathological processes *in vivo*. It is tempting to speculate that formation of leaders and outgrowths can be regarded as a simplified bidimensional analogue of 3D outgrowths from epithelial and endothelial structures that provide the basis for tubulogenesis and angiogenesis (reviewed in ref. 29). More generally, the molecular mechanisms involving Rho activities may provide a new basis for the old idea of controlling some aspects of morphogenesis by tension (30).

Lastly, abnormally increased activity of RhoA in RhoA Q563L transfectants facilitates detachment of individual cells into the fluid medium with further colonization onto cell-free substrata. This process can, possibly, model some stages of formation of metastasis by malignant tumors. For example, it has been suggested that increased Rho activity was responsible for Ras-induced morphologic neoplastic transformation (31). Alterations of Rho activity were also observed in various neoplastic tissues (reviewed in refs. 32–34).

We thank Dr. G. Bokoch (The Scripps Research Institute, La Jolla, CA) for providing plasmids and Dr. A. Ljubimov (Cedars-Sinai Medical Center, Los Angeles) for providing antibodies. Funding for this study was provided by a Russian Foundation of Basic Investigation grant and a Ludwig Foundation grant (to J.M.V.), by a gracious gift from Mrs. Harold Kaplan to the Research Exchange Program at Rutgers (Newark), and by a Johnson & Johnson Discovery Award (to E.M.B.).

1. Trinkaus, J. P. (1984) *Cells into Organs: The Forces that Shape the Embryo* (Prentice-Hall, Englewood Cliffs, NJ), 2nd Ed.
2. Kaltschmidt, J. A., Lawrence, N., Morel, V., Balayo, T., Fernandez, B. G., Plissier, A., Jacinto, A. & Arias, A. M. (2002) *Nat. Cell Biol.* **4,** 937–944.
3. Nodder, S. & Martin, P. (1997) *Anat. Embryol.* **195,** 215–228.
4. Wood, W., Jacinto, A., Grose, R., Woolner, S., Gale, J., Wilson, C. & Martin, P. (2002) *Nat. Cell Biol.* **4,** 907–912.
5. Ridley, A. J. (2001) *Trends Cell Biol.* **11,** 471–477.
6. Aelst, L. V. & Symons, M. (2002) *Genes Dev.* **16,** 1032–1054.
7. Kiehart, D. P., Galbraith, C. G., Edwards, K. A., Rickoll, W. L. & Montague, R. A. (2000) *J. Cell Biol.* **149,** 471–490.
8. Lu, Y. & Settleman, J. (1999) *Genes Dev.* **7,** 29–41.
9. Jacinto, A., Wood, W., Woolner, S., Hiley, C., Turner, L., Wilson, C., Martinez-Arias, A. & Martin, P. (2002) *Curr. Biol.* **12,** 1245–1250.
10. Montesano, R., Saint Vincent, L., Drevon, C. & Tomatis, L. (1975) *Int. J. Cancer* **16,** 550–558.
11. Subauste, M. C., Von Herrath, M., Benard, V., Chamberlain, C. E., Chuang, T. H., Chu, K., Bokoch, G. M. & Hahn, K. M. (2000) *J. Biol. Chem.* **275,** 9725–9733.
12. Belmont, A. S., Li, G., Sudlow, G. & Robinett, C. (1999) *Methods Cell Biol.* **58,** 203–222.
13. Uehata, M., Ishizaki, T., Satoh, H., Ono, T., Kawahara, T., Morishita, T., Tamakawa, H., Yamagami, K., Inui, J., Maekawa, M. & Narumiya, S. (1997) *Nature* **389,** 990–994.
14. Gloushankova, N. A., Alieva, N. A., Krendel, M. F., Bonder, E. M., Feder, H. H., Vasiliev, J. M. & Gelfand, I. M. (1997) *Proc. Natl. Acad. Sci. USA* **94,** 879–883.
15. Welnhofer, E. A., Zhao, L. & Cohan, C. S. (1997) *Cell Motil. Cytoskel.* **37,** 54–71.
16. Krendel, M., Gloushankova, N. A., Bonder, E. M., Feder, H. H., Vasiliev, J. M. & Gelfand, I. M. (1999) *Proc. Natl. Acad. Sci. USA* **96,** 9666–9670.
17. Gloushankova, N. A., Krendel, M. F., Sirotkin, V. A., Bonder, E. M., Feder, H. H., Vasiliev, J. M. & Gelfand, I. M. (1995) *Proc. Natl. Acad. Sci. USA* **92,** 5322–5325.
18. Worthylake, R. A., Lemoine, S., Watson, J. M. & Burridge, K. (2001) *J. Cell Biol.* **154,** 147–160.
19. Stoker, M., Gherardi, E., Perryman, M. & Gray, J. (1987) *Nature* **342,** 440–443.
20. Birchmeier, C. & Gherardi, E. (1998) *Trends Cell Biol.* **8,** 404–410.
21. Thiery, J. P. (2002) *Nat. Rev. Cancer* **2,** 442–452.
22. Omelchenko, T., Fetisova, E., Ivanova, O., Bonder, E. M., Feder, H., Vasiliev, J. M. & Gelfand, I. M. (2001) *Proc. Natl. Acad. Sci. USA* **98,** 8632–8637.
23. Omelchenko, T., Vasiliev, J. M., Gelfand, I. M., Feder, H. H. & Bonder, E. M. (2002) *Proc. Natl. Acad. Sci. USA* **99,** 10452–10457.
24. Krendel, M. F. & Bonder, E. M. (1999) *Cell Motil. Cytoskel.* **43,** 296–309.
25. Salmon, W. S., Adams, M. C. & Waterman-Storer, C. M. (2002) *J. Cell Biol.* **158,** 31–37.
26. Bershadsky, A. D., Vaisberg, E. A. & Vasiliev, J. M. (1991) *Cell Motil. Cytoskel.* **19,** 152–158.
27. Yvon, A.-M., Gross, D. J. & Wadsworth, P. (2001) *Proc. Natl. Acad. Sci. USA* **98,** 8656–8661.
28. Waterman-Storer, C. M., Worthylake, R. A., Liu, B. P., Burridge, K. & Salmon, E. D. (1999) *Nat. Cell Biol.* **1,** 45–50.
29. Zegers, M. M. P., O'Brien, L. E., Yu, W., Datta, A. & Mostov, K. E. (2003) *Trends Cell Biol.* **13,** 169–176.
30. Stopak, D. & Harris, A. K. (1982) *Dev. Biol.* **26,** 28–35.
31. Zhong, C., Kinch, M. S. & Burridge, K. (1997) *Mol. Biol. Cell* **8,** 2329–2344.
32. Sahai, E. & Marshall, C. J. (2002) *Nat. Rev. Cancer* **2,** 133–142.
33. Lozano, E., Betson, M. & Braga, V. M. M. (2003) *BioEssays* **25,** 452–463.
34. Clark, E. A., Golub, T. R., Lander, E. S. & Hynes, R. O. (2000) *Nature* **406,** 532–535.